

Research of the Behavior of Solar Module Frame Installed by Solar Clamping System by Finite Element Method

Li-Chung Su, Chia-Yu Chen, Tzu-Yuan Lai, and Sheng-Jye Hwang

Abstract—Mechanical design of the thin-film solar framed module and mounting system is important to enhance module reliability and to increase areas of applications. The stress induced by different mounting positions played a main role controlling the stability of the whole mechanical structure. From the finite element method, under the pressure from the back of module, the stress at Lc (center point of the Long frame) increased and the stresses at Center, Corner and Sc (center point of the Short frame) decreased while the mounting position was away from the center of the module. In addition, not only the stress of the glass but also the stress of the frame decreased. Accordingly it was safer to mount in the position away from the center of the module. The emphasis of designing frame system of the module was on the upper support of the Short frame. Strength of the overall structure and design of the corner were also important due to the complexity of the stress in the Long frame.

Keywords—Finite element method, Framed module, Mounting position

I. INTRODUCTION

THIN-FILM solar modules can be divided into framed and frameless ones according to the frame system. Using 3.2-5 mm float glass as substrate, depositing the photovoltaic layers including a-Si layer, then:

1. For the framed module, laminate polymer protecting materials such as backsheet and EVA to protect active area from the environment. The final step is to assemble buffer rubber and frame system to complete the module.
2. For frameless module, laminate tempered glass to protect active area from the environment.

According to IEC 61646 thin-film terrestrial photovoltaic (PV) modules - Design qualification and type approval [1], the normal and back side minimum mechanical load of the solar module is 2400Pa. Float glass is commonly used as the substrate of solar modules due to its great transparency and low cost. The deposition processes of the photovoltaic layers are always with high temperature, therefore, it is not easy using the

L.-C. Su is with the NexPower Technology CORP., Taichung 421, Taiwan, ROC (corresponding author to provide phone: 886-4-2580-8888 ext.1504; fax: 886-4-2580-8889; e-mail: chris_su@nexpw.com).

C.-Y. Chen is with the NexPower Technology CORP., Taichung 421, Taiwan, ROC (e-mail: jimmy_chen@nexpw.com).

T.-Y. Lai is with the NexPower Technology CORP., Taichung 421, Taiwan, ROC (e-mail: cooke_lai@nexpw.com).

S.-J. Hwang is with the Department of Mechanical Engineering, National Cheng Kung University, Tainan 701, Taiwan, ROC (e-mail: jimpp1@mail.ncku.edu.tw).

tempered or semi-tempered glass as the substrate. There are some approaches to enhance the mechanical strength of the module which comprises the brittle glass:

1. To increase the thickness of glass
2. To laminate with tempered glass
3. To laminate with protecting materials such as back-sheet/EVA to strengthen the module.
4. To design the module frame and the buffer rubber appropriately.

The total cost analysis of thin film solar module system is shown in Fig. 1. In which, 51 % of the cost is the solar module and frame of module, including the buffer rubber. Consequently, it is both helpful to decrease the cost of the module and to increase the competitiveness of the module. Besides, in Fig. 1, the substructure and installation cost is the second highest. As a result, if the framed system of the solar module can be easily handled and installed, the cost of the solar system can be dramatically reduced and the whole system will be more cost effective.

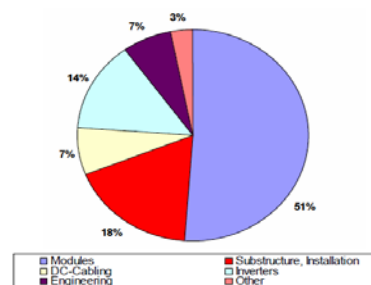


Fig. 1 Cost analysis of thin-film solar module system

This paper focused on the FEM simulations verified by experiments to analyze the behavior of framed module mounted at different positions under mechanical load in order to accomplish the highly reliable and applicable solar system structure. Due to its high transmittance and great strength, glass is widely used in industries, such as LCD, curtain wall and solar module. Also, glass is the main structure providing the strength within the solar module but the research about the mechanism affecting the strength of glass is rarely done. Glass is a brittle material so its fracture toughness is unpredictable under tensile stress. And the strength of glass depends on both geometry and loading[2]. Moreover, defects in glass cause stress concentration and the quantity of defects is directly proportional to the size of glass. These factors affect the tensile strength of glass dramatically.

The theoretical strength of glass is 14000MPa [3] but the actual one is unpredictable. The actual strength of glass can not be precisely calculated via any equations. Therefore this paper based on the FEM simulations and the results of experiments defines the stress limitation of glass and then makes it possible to develop a safer solar module.

The framed solar module was used as the analysis model and the assembly drawing of the modules and the mounting system was shown in Fig. 2. Dimensions of the module were $1412 \times 1112 \text{mm}^2$ and dimensions of the glass were $1400 \times 1100 \text{mm}^2$. When installing the framed module, it was fixed by clamp system. Transmission of force between the module and the system depended only on the contact area in between. The mechanical system should not only maintain the long term stability but also help the module to release the 2400Pa pressure. In Fig. 2, the character C represented the mounting position measured from the edge of module.

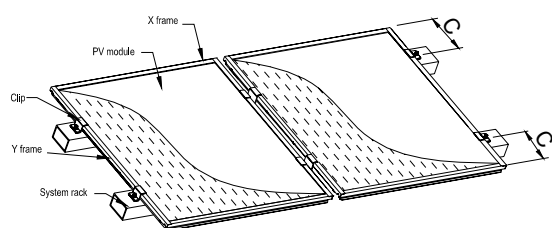


Fig. 2 Schematic drawing of solar modules and mounting system

II. EXPERIMENT

A. Standards

The experiments were following the standard of IEC 61646 thin-film terrestrial photovoltaic (PV) modules - design qualification and type approval. It includes visual inspection test, electrical test, irradiation test, environment test, and mechanical test. The standard lays down requirements for thin-film solar modules suitable for long-term operation in general open-air climates. The experiments of this paper were focusing on the mechanical load test to determine the ability of the module to withstand wind, snow, ice or static load.

B. Experiment Procedures

The module was installed on the system rack as shown in Fig. 3 and then the module and the rack were placed on the test platform. A uniform surface pressure, equivalent to 2400Pa applied via water, was applied onto the module, as shown in Fig. 4. The module was installed at the locations of $C=120\text{mm}$, 200mm , 350mm and 450mm to analyze the behavior of the module under loading. The vertical displacements of the module at the Center, Sc, Lc and the Corner were measured, as shown in Fig. 5. The mounting position was used as X-axis and the vertical displacement or the stress was taken as Y-axis in the following analysis.

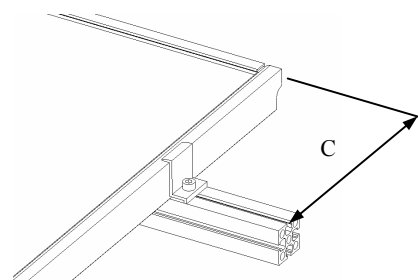
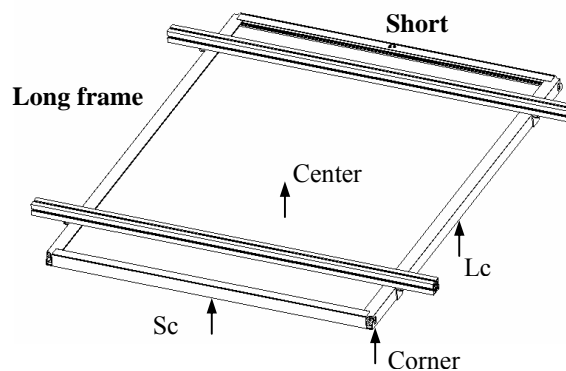


Fig. 3 Installation of module and system rack (C: mounting position)



Fig. 4 2400Pa water pressure applied on the module



Center: center point of glass
 Sc: center point of Short frame
 Lc: center point of Long frame
 Corner: corner point of module

Fig. 5 Measurement points of vertical displacement on the module

C. Experiment Results

The results of experiments were summarized in Fig. 6. The maximum displacement occurred at glass center and became larger while the mounting position was closer to the center of module. The trend was the same for the displacement at the Sc and Corner. But the displacement at the Lc showed the opposite trend.

The simulation results of vertical displacement to mounting positions were shown in Fig. 8 and it showed that simulation results matched very well with experiment results. For the mounting position at 350mm , the maximum error was 29.4% (Center). The simulation results fairly satisfied the expectation that the deformation of module could be predicted by FEM effectively.

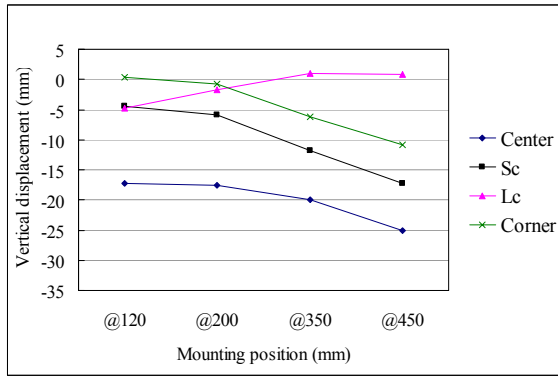


Fig. 6 Relation between the mounting position and the vertical displacements (experiment)

III. FINITE ELEMENT ANALYSIS

A. Simulation Model

As shown in Fig. 7, the model of framed module was built with quarter symmetry. Dimensions of the module were 1412x1112mm² and dimensions of the glass were 1400 x1100mm². Analysis type was static structural load and the behavior of the module was simulated under back load. The boundary condition was applied by back pressure (2400 Pa) onto the backsheet including projection area of system rack and the earth gravity was considered.

There were complicated contact pairs in the entire module. Under the premise of matching experiment results, the contact pairs were set as frictional pairs comprising frame with gasket, gasket with glass, and gasket with backsheet and frictionless pairs comprising frame with frame, frame with clamp and frame with system rack and bonded pairs comprising glass with EVA and EVA with backsheet.

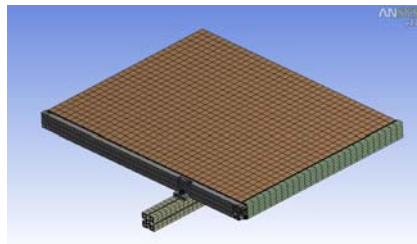


Fig. 7 Quarter symmetry FEM model of framed module

B. Simulation Results

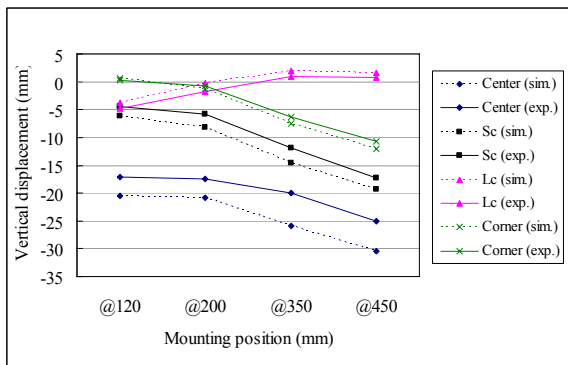


Fig. 8 Comparison of experiment and simulation results

1) Displacement Analysis

Short frame: Vertical displacement data was collected along line A (shown in Fig. 9) and the results were shown in Fig. 10. It could be expected that the displacement increased when clamps were mounted toward the center of Long frame.

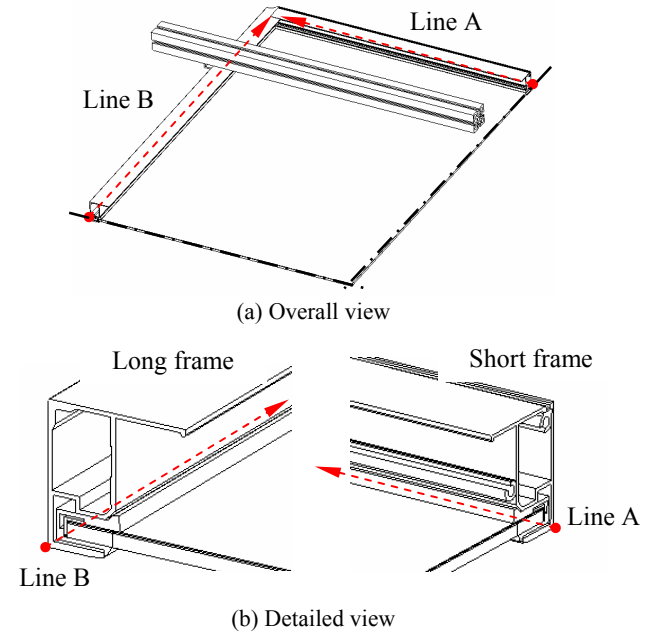


Fig. 9 Analysis along line A in Short frame and line B in Long frame

The deflection of Short frame versus mounting position was shown in Table I. The bending direction was the same. All of them bend upward (positive bending) and the displacement increased when clamps were mounted toward the center of Long frame. Short frame was connected to Long frame through screws only. That meant Short frame resisting the bending force by the strength of overall structure of itself. With the increase of deflection, the overall stress of Short frame would also increase.

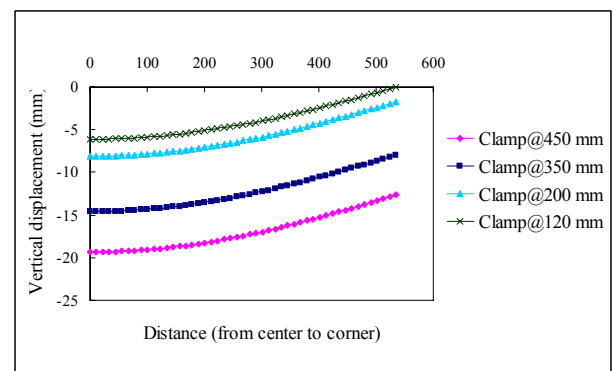


Fig. 10 Vertical displacement of Short frame along line A when installed in different mounting positions

TABLE I
 DEFLECTION OF SHORT FRAME

Mounting positions C (mm)	120	200	350	450
Deflection (mm)	+6.10	+6.36	+6.64	+6.71

Long frame : Vertical displacement data was collected along line B (shown in Fig. 9) and the results were shown in Fig. 11. The deformation mechanism of Long frame was constrained by clamps. The frame had positive and negative displacements away from the clamps and was back to about zero around the clamps (because clamp also deformed under load). Because there were clamps supporting Long frame, one could find that the behavior of the Long frame was different when clamps were mounted at $C > 200\text{mm}$ or $C < 200\text{mm}$. Long frame was under negative bending moment when clamps were mounted at $C > 200\text{mm}$. Under this case, the displacement of center of Long frame was upward and the corner was downward. Long frame was under positive bending moment when clamps were mounted at $C < 200\text{mm}$. Under this case, the displacement of center of Long frame was downward and the corner was upward. The behaviors of Long frame when clamps were mounted at different positions were shown in Table II.

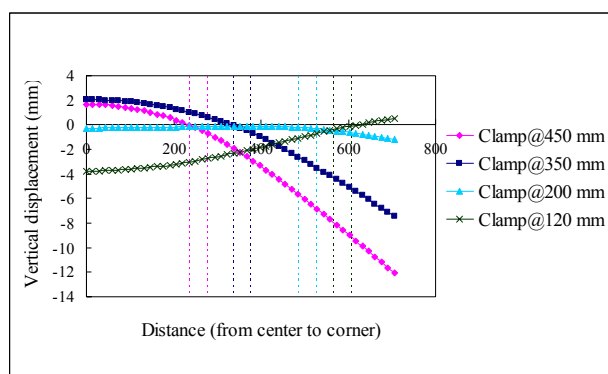


Fig. 11 Deflection of Long frame along line B when installed in different mounting positions

TABLE II
 DEFLECTION OF LONG FRAME

Mounting positions C (mm)	120	200	350	450
Deflection (mm)	+4.30	-1.07	-9.45	-13.73

2) Strain and Stress Analysis

Short frame : Stress distribution of frame was calculated with equivalent stress. High stress was concentrated on upper plate of Short frame when clamps were mounted at 200mm, as shown in Fig. 12. The stress distribution was acquired along line A (Fig. 9) and the results were shown in Fig. 13. High stress was induced near the center of Short frame and it implied that there was also high strain level induced. Fig. 14 showed the normal strain distribution on Short frame when clamps were mounted at 200mm.

Regarding stress distribution versus different mounting

positions, stress increased when clamps were mounted towards the center of Long frame. The maximum stress values and locations were shown in Table III. Consequently, the design of Short frame should emphasize on upper plate structure.

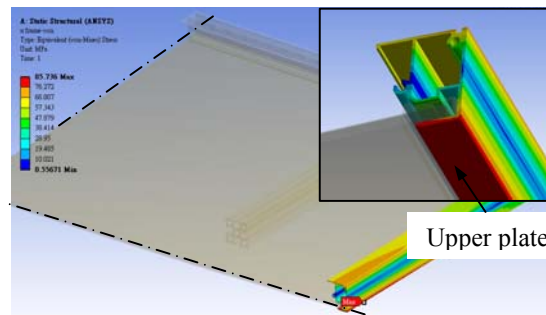


Fig. 12 Equivalent stress of Short frame (when C=200mm)

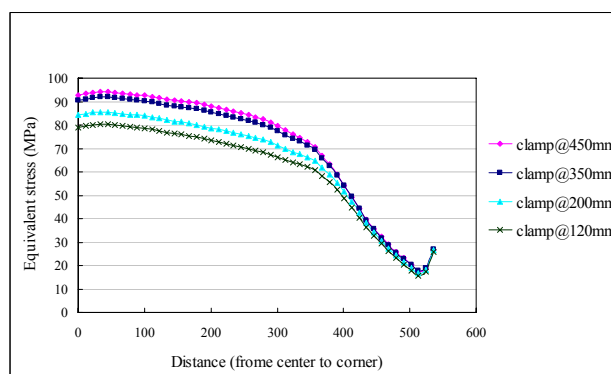


Fig. 13 Stress distribution of Short frame along line A when installed in different mounting positions

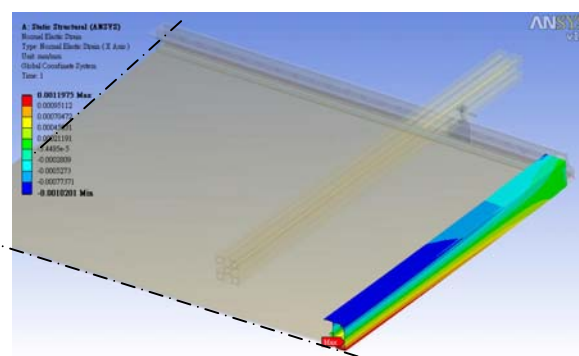


Fig. 14 Normal strain of Short frame (when C=200mm)

TABLE III
 STRESS DISTRIBUTION OF SHORT FRAME UNDER DIFFERENT MOUNTING POSITIONS

Mounting positions C (mm)	120	200	350	450
Max. stress (MPa)	80.36	85.59	91.91	94.16
Location	Upper plate	Upper plate	Upper plate	Upper plate

Long frame: Long frame had more complex behavior under load. The stress was affected by two main factors. One was that

the stress was induced by clamps as shown in Fig. 15. The stress distribution acquired along line B shown in Fig. 16 showed that the maximum stress occurred where the frame was constrained by clamps. There was more stress induced when clamps were mounted toward the center of Long frame. The maximum stress corresponding to different mounting positions was shown in Table IV. When clamps were mounted at 450mm, the maximum stress of Long frame was 130.38MPa which was much higher than that of Short frame while clamps were mounted at any positions. As a result, if one wanted to mount clamps at 450mm or even closer to the center of Long frame, more consideration should be taken on Long frame than Short frame from overall stress point of view. In addition, the stress of Long frame at locations where clamp was mounted was smaller than that at center when the clamps were mounted at 120mm. The deformation mechanism of Long frame had changed when clamps were mounted at $C < 200$ mm. When clamps were mounted at 120mm or closer to the corner, the overall structure strength was strong enough because the safety factor was more than two. Meanwhile the simulation results showed that the stress at corner increased gradually. The stress occurred at corner was the second factor affecting stress distribution of frame as shown in Fig. 16(see dash circle). The high stress was induced at corner due to the deformation of Short frame under load. (refer to the red symbol in Fig. 15) The maximum stress at corner was 164.5MPa and occurred at the edge of the hollow area. When designing Long frame, one could summarize that both reducing the overall stress of frame and improving the stress level at specific locations were very critical and worth further research.

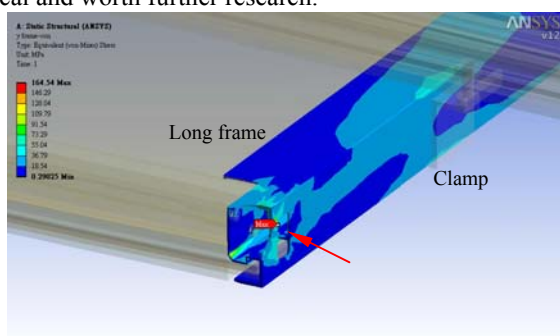


Fig. 15 Equivalent stress of Long frame (when C=200mm)

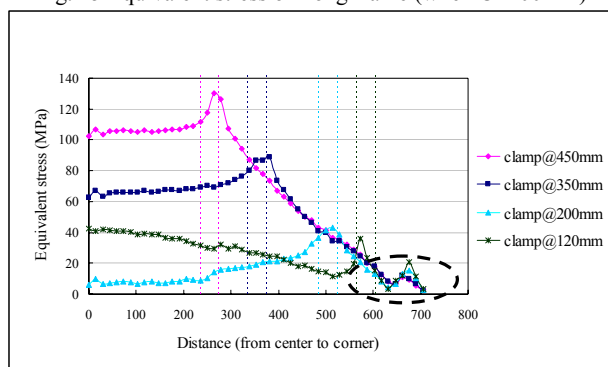


Fig. 16 Stress distribution of Long frame along line B when installed in different mounting positions

TABLE IV
 STRESS DISTRIBUTION OF LONG FRAME UNDER DIFFERENT MOUNTING POSITIONS

Mounting positions C (mm)	120	200	350	450
Stress (MPa)	35.81	42.92	89.05	130.38

Glass : Stress distribution of glass was calculated with maximum principal stress. Maximum stress of glass was 31.86MPa and occurred at the front surface when clamps were mounted at 200mm, as shown in Fig. 17. Glass stress corresponding to clamps mounting positions was summarized in Table V. The results showed glass stress was affected by clamp mounting position and decreased when clamps were mounted toward the outer edge of the Long frame.

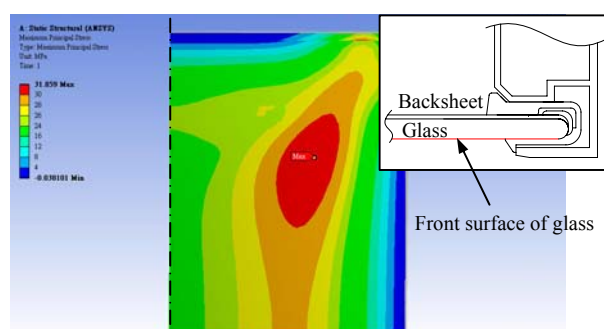


Fig. 17 Maximum principal stress of front surface of glass (when C=200mm)

The failure of brittle materials is mainly due to tensile failure. In other words, the material will be failed if the tensile stress exceeds fracture strength. High tensile stress occurred at front surface of glass under back load, therefore decreasing stress at front surface was very important to improve module structure reliability.

The strength of glass depends on both geometry dimensions and loading methodologies. One could confirm that the whole system was safe when clamps were mounted at 120mm-450mm through experiments. In the meantime, FEM results showed the maximum glass stresses were between 29MPa and 41MPa, as shown in Table V. As a result, the values in Table V indicated the capable stress of glass and could be defined as design rules for future development. On the other hand, it was also critical to reduce high stress area to get more robust structure strength.

TABLE V
 MAXIMUM PRINCIPAL STRESS OF GLASS

Mounting positions C (mm)	120	200	350	450
Max. stress (MPa)	29.14	31.86	38.25	41.39

IV. CONCLUSIONS

The overloaded failures of framed module were due to two factors. One was that the strength of frame was insufficient and the other was that the stress induced exceeded the strength of

glass.

The insufficiency of frame strength was from the weak Short frame or Long frame. Lack of Long frame strength could be imputed to weak overall structure or weak design at critical location such as corner. Because of the different deformation mechanisms for both Short frame and Long frame, one should focus on different improvements for them. The Short frame resisted the bending force by the strength of overall structure and the induced stress concentrated on upper plate of Short frame so the emphasis should be placed on the enhancement of the feature. There was more complex stress distribution on Long frame under load. The localized high stress caused by the mounting clamps and the corner stress induced by the deformation of Short frame should be both improved. The former could be overcome by increasing the overall structural strength of Long frame. The latter could be improved by the optimization of the local geometry at the corner.

Besides increasing the thickness, the corner of Long frame would not only be improved by enlarging the radius of corner but also by making more contact area with Short frame to release the stress concentration.

In this research, the simulation results indicated that the stresses of glass, Short frame, and Long frame were all decreased when clamps were mounted toward the outer edge of the Long frame which meant the module was safer and more robust.

Because the contact conditions of the simulation had not met the actual situation exactly yet, the issue of the stress at the joint of Short frame and Long frame remained unclear. Further research to make it more complete is recommended.

REFERENCES

- [1] IEC61646, Thin-film terrestrial photovoltaic (SOLAR) modules – Design qualification and type approval, 2008.
- [2] F. Veer, J. Zuidema, F.P. Bos, The strength and failure of glass in bending. Glass processing days, 2005.
- [3] E. K. PAVELCHEK, R. H. OREMUS, Fracture strength of soda-lime glass after etching. Journal of Materials Science, vol. 9, pp. 1803-1808, 1974.